

## Selective Laser Sintering of SiC/Polyamide Matrix Composites

Toby Gill and Bernard Hon  
Rapid Prototyping Centre  
Department of Engineering, The University of Liverpool, Uk.

### Abstract

This paper presents an experimental study into the production of particulate Silicon Carbide/Duraform Polyamide matrix composites via the selective laser sintering (SLS) process. FEPA standard SiC grits, F240 and F360, were each individually blended with the commercially available Duraform Polyamide, to produce blend compositions of 50 and 60 volume percent SiC for direct SLS processing. A full factorial experimental approach was applied to examine the effects and interactions of laser power, scan speed, scan spacing and layer thickness, with regards to the mechanical and physical properties of sintered parts. Analysis of parameter interactions and individual main effects as well as Pareto analysis for all parameter combinations are presented for the responses of part porosity and strength.

### Introduction

SLS is a solid freeform fabrication (SFF) technique that was originally developed at the University of Texas at Austin and commercialised by DTM Corporation (now part of 3D Systems) between 1987 and 1992 [1]. Since the sale of the first commercial system in 1992 there has been continued development with regards to machine capabilities as well as commercially available materials. This continued development has led to a wide range of applications from conceptual models, functional prototypes, patterns for casting, through to rapid manufacturing (RM), and industrial sectors using SLS produced parts, range from military to medical. For example, the International Space Station is equipped with hundreds of glass-filled nylon retainers, sintered ducts have been produced for the space shuttles engines and SLS is also being applied as a means for producing custom hearing aids [2,3].

Despite the advancements made, there are still only a few commercially available materials for use with SLS systems [4]. Yet the process gives virtually unlimited material choice compared to most other SFF technologies, and basically any material that can be pulverized may be employed [5]. The SLS of ceramics (SiC and Al<sub>2</sub>O<sub>3</sub>) has been investigated in the past and various binders (e.g. PMMA, Aluminium) have been utilised for the production of parts. Interest in these ceramics has been due to the desire for fully functional prototypes, which are suitable for application testing and also for the production of investment casting moulds and preforms [6,7,8]. To develop a new and novel material system the SLS of SiC/Polyamide matrix composites is being researched at the University of Liverpool. In this process a ceramic powder is mixed with a polymer material that acts as the bonding system, and then laser sintered to form a 3-D object. The current materials being used are FEPA (Federation of the European Producers of Abrasives) standard silicon carbide grits F240 and F360, each individually blended with the commercially named Duraform Polyamide (3D Systems). Some of the specifications for the commercially supplied powders are listed in Table 1 and Figure 1 shows a micrograph of the powder particles.

	F240	F360	Duraform Polyamide
<b>Mean Diameter (<math>\mu\text{m}</math>)</b>	$44.5 \pm 2.0$	$22.8 \pm 1.5$	58
<b>Particle Size range (<math>\mu\text{m}</math>)</b>	28 - 70	12 - 40	25 - 92
<b>Particle Shape</b>	Irregular	Irregular	Irregular
<b>Solid Density (<math>\text{g}/\text{cm}^3</math>)</b>	3.2	3.2	0.97
<b>Melting Temp (<math>^\circ\text{C}</math>)</b>			186

**Table 1.** Material specifications (3D Systems and Washington Mills).

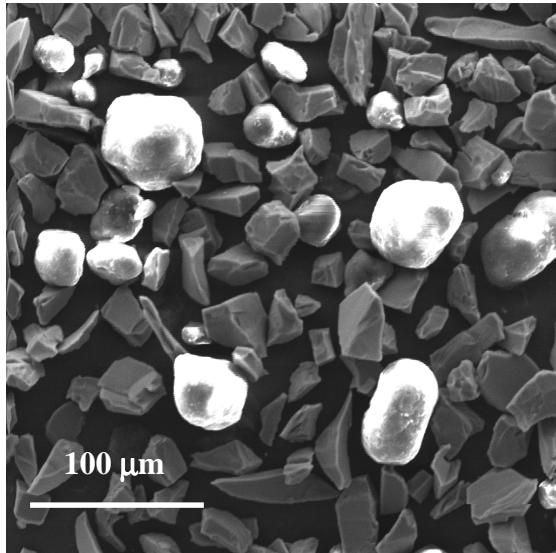


**Figure 1.** Micrograph showing F360 SiC and Duraform Polyamide.



**Figure 2.** Experimental chamber, single feed with reduced build and feed chamber.

When developing a new material system for SLS processing it is important to understand individual effects and the interactions that may occur between fabrication parameters. It is known that material properties and fabrication parameters have a great influence on the mechanical properties of SLS parts. Fill laser power (P) can be approximately calculated for a given material by the following equation [9].

$$P = \frac{BS \cdot \rho \cdot Db \cdot LT \cdot [C \cdot (Tm - Tb) + Lf]}{(1 - R)} \quad (1)$$

Where  $BS$  is beam Speed,  $\rho$  is powder bed density,  $Db$  is diameter of laser beam,  $LT$  is layer thickness,  $C$  is specific heat,  $Tm$  is melting temperature,  $Tb$  is bed temperature,  $Lf$  is latent melting heat and  $R$  is reflectivity. Fill laser power and beam speed along with scan spacing (SCSP) also determines the energy density [10], which corresponds to the incident energy at the surface of the part bed. Energy density has been shown to have a significant effect on the overall part quality [9, 10].

$$\text{EnergyDensity}(\text{J} / \text{mm}^2) = \frac{P \cdot f}{BS \cdot SCSP} \quad (2)$$

From equations (1) and (2) it can be seen that the main fabrication parameters (in terms of energy delivered) that influence the SLS process are  $P$ ,  $BS$ ,  $SCSP$  and  $LT$  along with material properties and laser beam spot size. Therefore it was decided to examine the effects and interaction of these four parameters with respect to part strength and porosity applying a two-level full factorial approach. The main advantages of a full factorial experiment are that, the response results can be combined to estimate the effects of individual and parameter combinations, whilst also estimating the interactions between the factors, and that they are the most efficient way of estimating individual parameter main effects [11].

## Experimental Procedure

Experiments were conducted on a Sinterstation 2000 system equipped with a 50 watt CO<sub>2</sub> laser, using a reduced feed chamber and build platform and with the machine capability for a single feed layer pass (Figure 2). Initial screening experiments had been evaluated to determine level settings, which were suitable for the investigation (Table 2), and a full factorial two-level experiment (Table 3) was designed using Minitab statistical and graphical analysis software package.

For the porosity analysis cuboids (5x5x10mm) were produced, as shown in Figure 3, and porosity was determined via a thermal binder burnout process. This method for examining porosity also yielded results with respect to compositional variation (not presented here). For Tensile strength analysis parts approximately half the geometry of the ISO 3167 standard multipurpose test specimen were SLS processed and tested in accordance with ISO 527 on an Instron 4505 at a test speed of 5mm/min, Figure 4 shows a part after failure.

Variable	Units	Low Level (-)	High Level (+)
P	Watts	4	8
BS	mm/s	1000	1250
SCSP	mm	0.15	0.2
LT	mm	0.1	0.125

Table 2. Variable Levels



Figure 3. Porosity cuboid



Figure 4. Tensile part

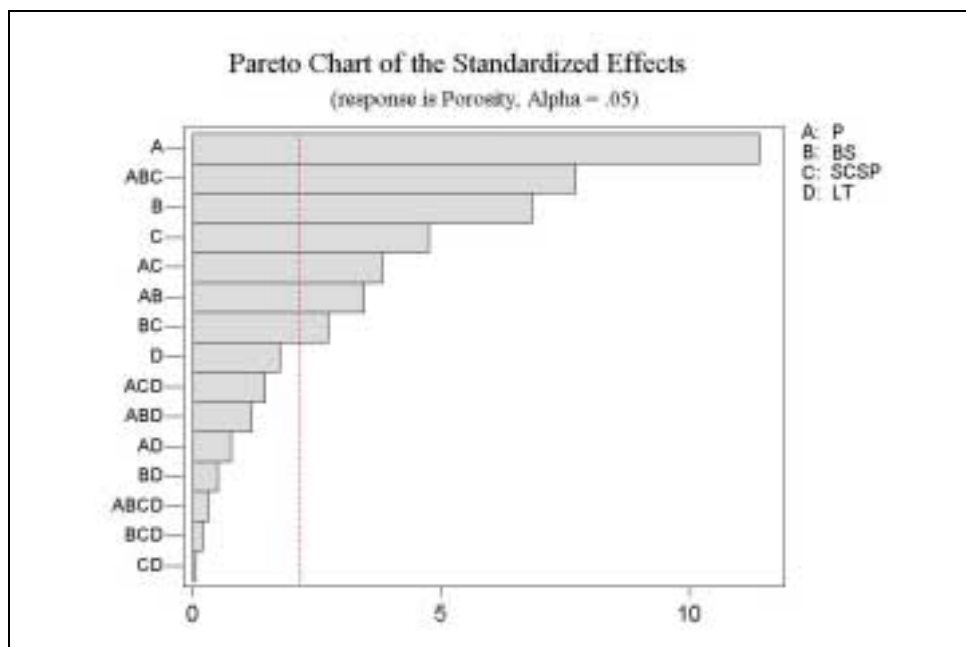
Test	Fabrication Parameter			
	P	BS	SCSP	LT
1	-	-	-	-
2	+	-	-	-
3	-	+	-	-
4	+	+	-	-
5	-	-	+	-
6	+	-	+	-
7	-	+	+	-
8	+	+	+	-
9	-	-	-	+
10	+	-	-	+
11	-	+	-	+
12	+	+	-	+
13	-	-	+	+
14	+	-	+	+
15	-	+	+	+
16	+	+	+	+

Table 3. Test Matrix

## Results and Discussion

In this section, some of the graphical outputs from the test results are presented with respect to part porosity and tensile strength. Minitab was again used to process the data, identifying significant effects and interactions and also significant parameter combinations. The results presented are focused on the 50-volume % F240 SiC/Duraform Polyamide powder blend. For all other blend compositions it was found that main effects were approximately equivalent, though sensitivity to fabrication parameter settings was increased with increasing SiC content.

One method available in Minitab for displaying the important process variables is to use a Pareto chart. The Pareto chart for porosity in the SLS produced cuboids is shown in Figure 5. The graphical summary displays the estimated effects in decreasing order of magnitude for factors both individually and combined, the length of each bar being proportional to the standardized effect. The vertical line represents the 95% confidence level and therefore bars extending beyond the line correspond to effects that are statistically significant.



**Figure 5.** Pareto chart for porosity in the SLS processed cuboids.

For the case of porosity it can be seen that 7 effects are statistically significant, consisting of three individual effects and interactions of laser power, beam speed and scan spacing. The single most influential fabrication parameter is laser power followed by the combination of parameters that yield the energy density (2). Three interactions of fabrication parameters are significant, laser power/scan spacing, laser power/beam speed and beam speed/scan spacing in order of rank.

From experiments reported by Gibson and Shi [9], where it is shown that the tensile strength is proportional to part density, then it would be expected that the Pareto chart for the response tensile strength would be similar to that for porosity. This was found to be the case with all 7 parameters that were statistically significant in terms of porosity being of similar importance in terms of tensile strength (Figure 6). There were slight variations with the singular most influential effect deriving from the interaction between laser power and scan spacing.

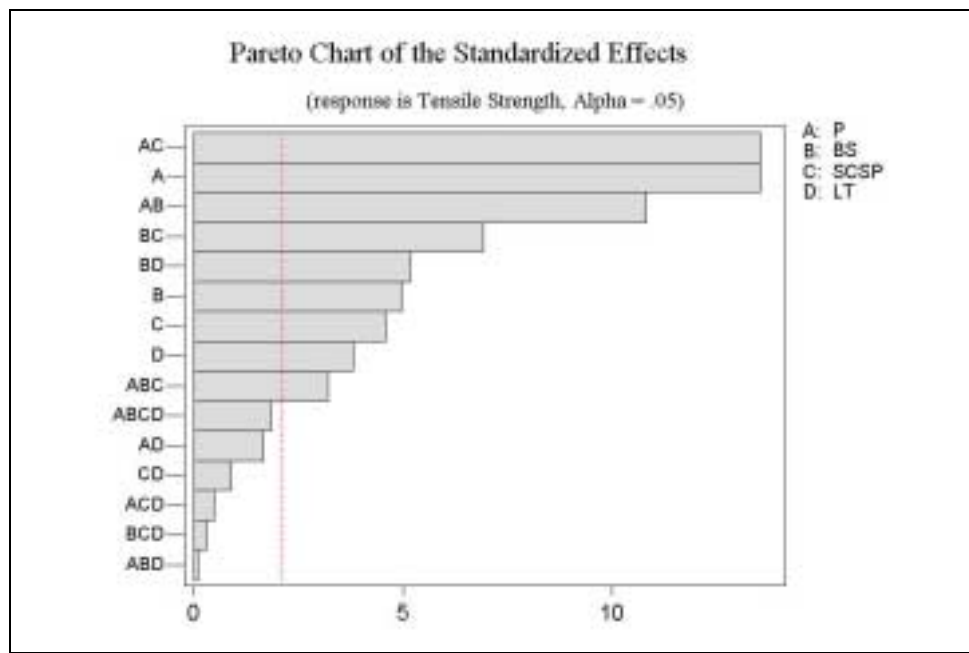


**Figure 6.** Pareto chart for tensile strength in the SLS processed parts.

Also it is noted that the layer thickness, although not important in terms of porosity, is in terms of tensile strength. A reason for this could be that as layer thickness increases, not enough energy is being delivered to the powder bed surface and therefore full melting of the polyamide is not achieved, which in turn will affect part strength more significantly than part porosity. SEM analysis has indicated that this may be the case though further investigation is required.

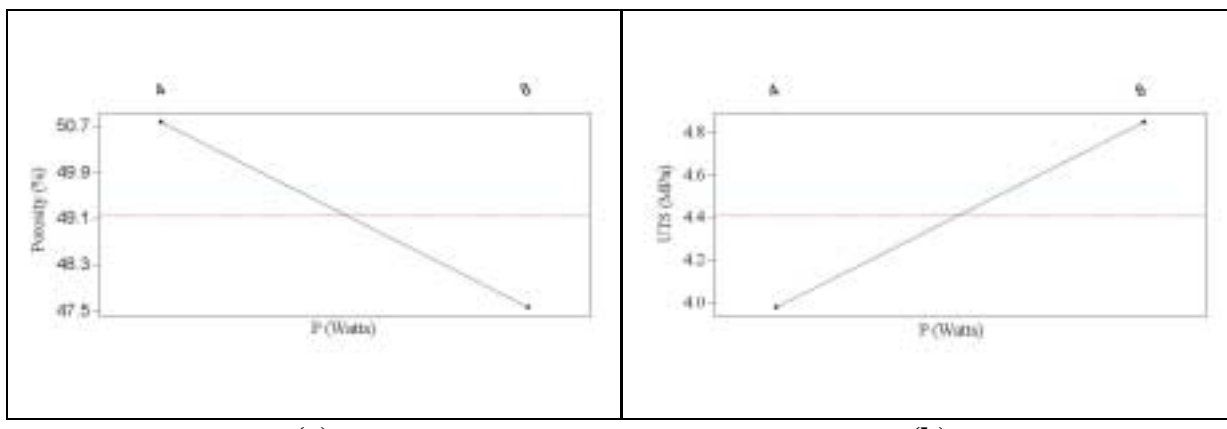


**Figure 7.** Main effects plot (data means) for response (a) porosity and (b) tensile strength with respect to laser power.

Figures 7 & 8 show the effects of laser power and scan spacing for the responses, porosity and tensile strength. The plot represents the average response obtained for parts built at that specific parameter level independent on other variable settings, with the line representing the magnitude and positive/negative effect of changing the individual parameter. Figure 7a shows that as laser power is increased the porosity decreases, with the estimated effect of changing laser power from 4 to 8 Watts being a decrease in porosity of approximately 3.2%. Figure 7b shows

that the effect of laser power in terms of part strength is the opposite too that for porosity, with tensile strength increasing by approximately 20%. Figures 8a & 8b show the effect of changing scan spacing and it can be seen that increasing scan spacing has the opposite effect, with a lesser magnitude when compared with increasing laser power for both porosity and tensile strength. In terms of porosity the effect of changing scan spacing from 0.15 – 0.2 mm is an increase of 2.3% and with respect to tensile strength a decrease of 6%. A similar trend was found for beam speed with porosity increasing by 2 % and tensile strength decreasing by 7% when increasing scan speed from 1000 to 1250 mm/s. Layer thickness as shown by the Pareto chart has little significance in terms of part porosity but has the same effect as scan spacing and beam speed with regards to tensile strength causing a decrease of 5% when increasing from 0.1 to 0.125 mm.

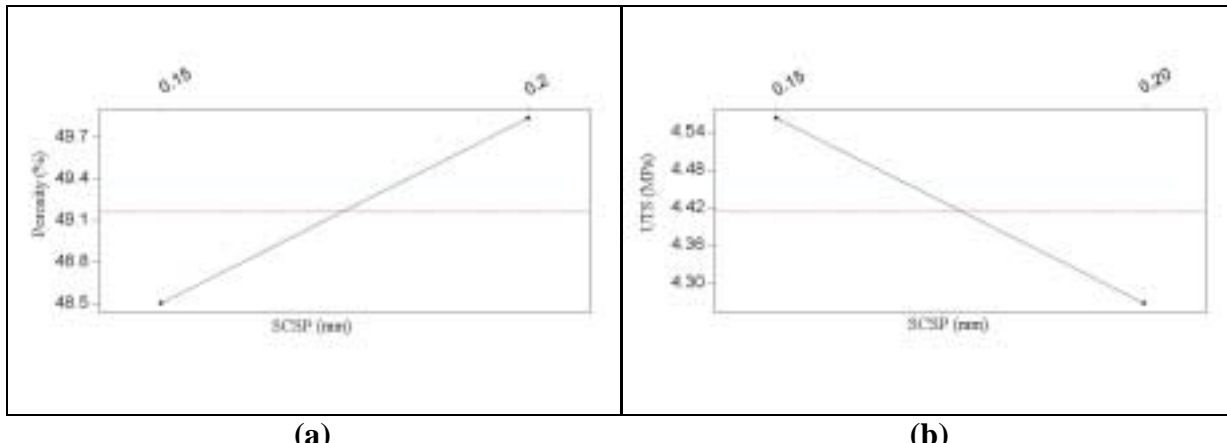


**Figure 8.** Main effects plot (data means) for response (a) porosity and (b) tensile strength with respect to scan spacing.

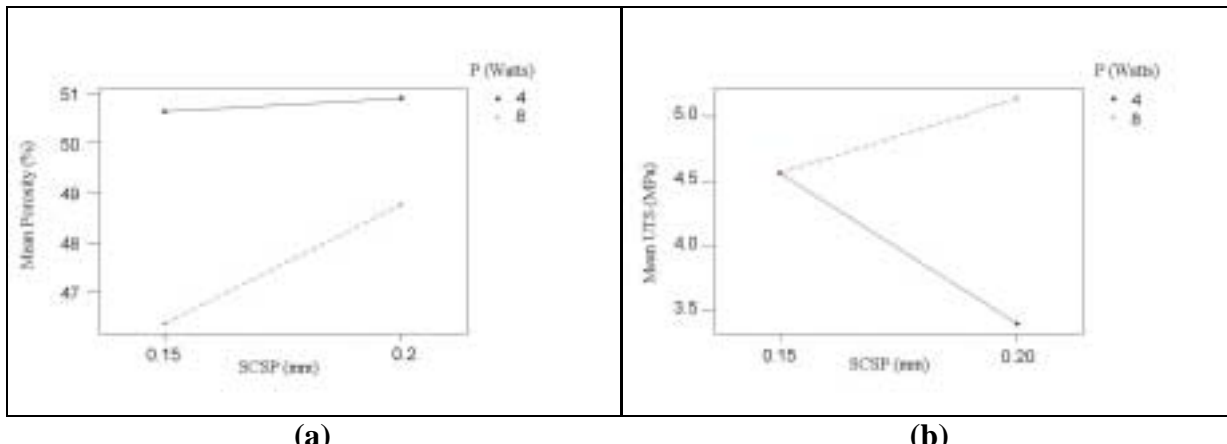


**Figure 9.** Interaction plot (data means) for response (a) porosity and (b) tensile strength with respect to laser power and scan spacing.

Figures 9, 10 & 11 show interaction plots for the three most significant fabrication parameter interactions. The interaction plot represents the average response obtained for parts built at the two defined fabrication parameter settings independently of the other variables. For example the average response for parts built at a laser power of 4 Watts and a scan spacing of 0.15 mm, with the line representing the magnitude and direction of the effect of increasing scan

spacing whilst laser power remains constant. Figure 9a shows that the interaction between laser power and scan spacing with respect to part porosity is moderate (i.e. lines skewed), were the effect of increasing scan spacing is to increase part porosity regardless of laser power setting. In terms of tensile strength (Figure 9b) there is a significant interaction effect with lines almost crossing, this was expected due to the significance of this interaction displayed in the Pareto chart. It is believed that at low laser power there is not enough incident energy to fully melt the polyamide, therefore greater overlap is required to ensure sufficient bonding between adjacent laser scan tracks. This problem may be magnified due to the tensile stress being in a direction perpendicular to the scan vector and hence the scan overlap. It is believed this may have a similar effect to stressing in the direction of layer thickness as outlined in [9]. At a higher laser power and small scan spacing too much energy is being delivered causing vaporisation of the polymer, therefore reducing binder content, which results in weaker parts.

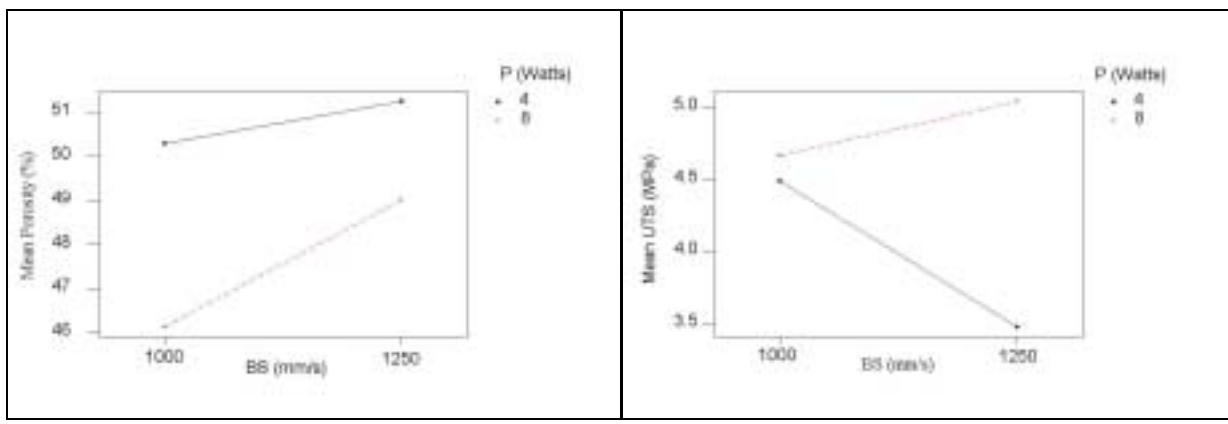


**Figure 10.** Interaction plot (data means) for response (a) porosity and (b) tensile strength with respect to laser power and beam speed.

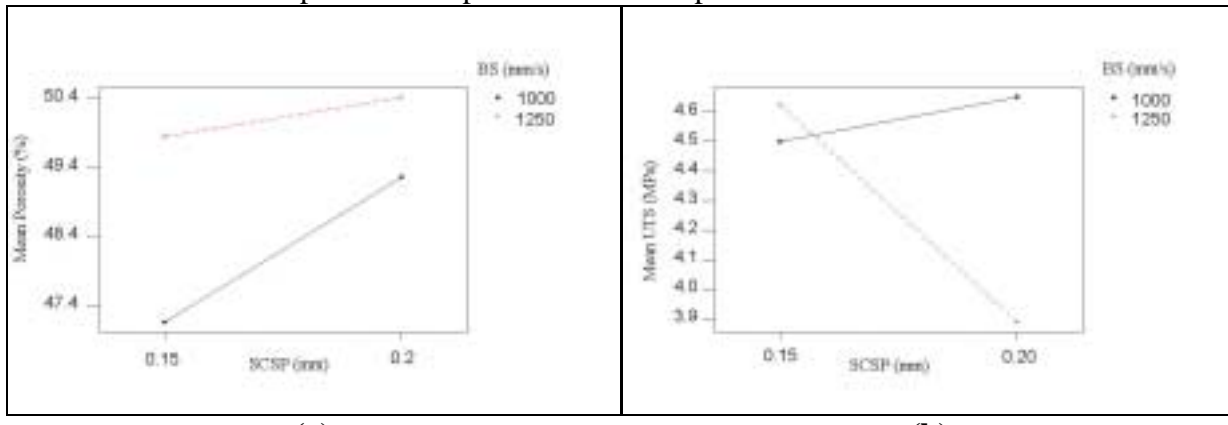


**Figure 11.** Interaction plot (data means) for response (a) porosity and (b) tensile strength with respect to beam speed and scan spacing.

Figures 10 & 11 are similar to Figure 9 with the interactions between beam speed/laser power and scan spacing/beam speed being less significant with regards to part porosity when compared with part strength. This agrees with the findings from the Pareto analysis. The same series of experiments have been investigated for varying compositions of initial powder blends

the results of which indicate that the effects of the 4 fabrication parameters are independent of material composition. However it was found that the interactions between parameters were more pronounced with reduced polyamide content indicating that sensitivity to the energy delivered increased.

## Conclusions

On performing a full factorial design of experiments approach with statistical graphical analysis into the selective laser sintering of SiC/Polyamide composites several conclusions were drawn. The selective laser sintering process is complex, with part porosity and strength being dependant not only on the individual parameter settings but also on the interactions and combination of fabrication parameters. Part porosity was inversely proportional to the tensile strength and it was shown that the significant parameter effects are similar for both cases. The major difference in terms of the two responses analysed were that parameter interactions were greatly increased with regards to the tensile strength. Further work into the effect of compositional variation is being investigated to explain the variation in interaction effects.

## Acknowledgement

The authors would like to acknowledge the financial support from the EPSRC and the technical support and assistance of the PIDC.

## References

1. J. J. Beaman, J. W. Barlow, D. L. Bourell, R. H. Crawford, H. L. Marcus, K. P. McAlea, Solid Freeform Fabrication – A New Direction in Manufacturing, Kluwer Academic Publishers, 1997.
2. T. Wohlers, “Rapid Manufacturing”, Computer Graphics World, November 2001.
3. M. Masters, M. Mathey, “Direct Manufacturing of Custom-made Hearing Instruments and Implementation of Digital Mechanical Processing”, Rapid Prototyping and Manufacturing Conference, Cincinnati, Ohio, 2002.
4. 3D Systems - [www.3dsystems.com](http://www.3dsystems.com)
5. D T Pham, R S Gault, “A Comparison of Rapid Prototyping Technologies”, Int. Journal of Machine Tools & Manufacture, vol. 38, 1998, pp 1257-1287.
6. T Srinivasa Rao, D L Bourell, H L Marcus, “Densification Behaviour of SLS Processed  $\text{Al}_2\text{O}_3/\text{Al}$  Composite”, SFF, 1995, pp 374-380.
7. U Lakshminarayan, S Ogrydziak, H L Marcus, “Selective Laser Sintering of Ceramic Materials”, SFF, 1990, pp 16-25.
8. N K Vail, J W Barlow, H L Marcus, “Silicon carbide Preforms for Metal Infiltration by Selective Laser Sintering™ of Polymer Encapsulated Powders”, SFF, 1993, pp 204-214.
9. I. Gibson, D. Shi, “Material Properties and Fabrication Parameters in Selective Laser Sintering Process”, Rapid Prototyping Journal, vol. 3, no. 4, 1997, pp 129-136.
10. J. C. Nelson, N. K. Vail, J. W. Barlow, J. J. Beaman, D. L. Bourell, H. L. Marcus, “Selective Laser Sintering of Polymer-Coated Silicon Carbide Powders”
11. C. Chatfield, Statistics for Technology – A Course in Applied Statistics, Chapman & Hall, 1983.